Atypical Developmental Trajectory of Functionally Significant Cortical Areas in Children with Chromosome 22q11.2 Deletion Syndrome

Siddharth Srivastava,[1,2]* Michael H. Buonocore,[1,3] and Tony J. Simon[1,2]

[1]*M.I.N.D. Institute, 2825, 50th Street, Sacramento, California*
[2]*Department of Psychiatry, U.C. Davis Medical School, Sacramento, California*
[3]*Imaging Research Center, U.C. Davis Medical Center, Sacramento, California*

◆ ━━━━━━━━━━━━━━━━━━━━━━━━━━━━━━ ◆

Abstract: Chromosome 22q11.2 deletion syndrome (22q11.2DS) is a neurogenetic disorder associated with neurocognitive impairments. This article focuses on the cortical gyrification changes that are associated with the genetic disorder in 6–15-year-old children with 22q11.2DS, when compared with a group of age-matched typically developing (TD) children. Local gyrification index (lGI; Schaer et al. [2008]: IEEE Trans Med Imaging 27:161–170) was used to characterize the cortical gyrification at each vertex of the pial surface. Vertex-wise statistical analysis of lGI differences between the two groups revealed cortical areas of significant reduction in cortical gyrification in children with 22q11.2DS, which were mainly distributed along the medial aspect of each hemisphere. To gain further insight into the developmental trajectory of the cortical gyrification, we examined age as a factor in lGI changes over the 6–15 years of development, within and across the two groups of children. Our primary results pertaining to the developmental trajectory of cortical gyrification revealed cortical regions where the change in lGI over the 6–15 years of age was significantly modulated by diagnosis, implying an atypical development of cortical gyrification in children with 22q11.2DS, when compared with the TD children. Significantly, these cortical areas included parietal structures that are associated, in typical individuals, with visuospatial, attentional, and numerical cognition tasks in which children with 22q11.2DS show impairments. *Hum Brain Mapp 33:213–223, 2012.*   © **2011 Wiley Periodicals, Inc.**

Key words: 22q11.2DS; development; cortex; gyrification; impairment

◆ ━━━━━━━━━━━━━━━━━━━━━━━━━━━━━━ ◆

INTRODUCTION

Chromosome 22q11.2 deletion syndrome (22q11.2DS) is a neurogenetic disorder having an estimated prevalence of one in 1600–3000 live births [Kobrynski and Sullivan, 2007; Shprintzen, 2008]. The phenotypy of 22q11.2DS is highly diverse and includes physical anomalies and cognitive impairments [Shprintzen, 2000; Simon et al., 2007] and increased risk for psychiatric disorders [Feinstein et al., 2002; Gothelf et al., 2007]. A direct neurobiological link between diminished chromosome 22q11.2 genes dosage and disrupted neurogenesis and migration in a mouse model was recently experimentally demonstrated [Meechan et al., 2009], suggesting alterations to cortical circuitry, connectivity, and increased risk for psychiatric disorders such as schizophrenia. Welker [1990] also noted that the deleted 22q11.2 genes would normally have been involved in establishing appropriate local differences in thickness, surface area, and gyral patterns of the cortex

during development. Further, Van Essen's [1997] neuro-mechanical hypothesis postulates that local cortico–cortico connectivity determines gyrification, providing a hypothetical link between the deletion, the connectivity alterations, and altered cortical gyrification in children with 22q11.2DS.

Brain imaging analysis, used independently or together with functional cognitive measures, has helped to provide quantitative evidence supporting the hypothesis of the association between genes and brain structure, connectivity, and function in 22q11.2DS. Alteration in gross brain measures, such as total brain, gray (GM), and white (WM) matter volumes [Eliez et al., 2000; Kates et al., 2001], has been reported in individuals with 22q11.2DS and in children with 22q11.2DS showing differences predominantly along the more medial aspects of the brain [Campbell et al., 2006; Simon et al., 2005, 2008]. Scalars, such as fractional anisotropy (FA), derived from diffusion tensor imaging (DTI) have indicated specific alterations in connectivity in children with 22q11.2DS [Barnea-Goraly et al., 2003; Simon et al., 2005]. Parietal connectivity differences correlate with impaired performance on spatial attention and arithmetical tasks [Barnea-Goraly et al., 2005; Simon et al., 2008]. Midline and parietal volumetric and connectivity alterations in 22q11.2DS, along with other cortical structures, colocalize with regions of reduced cortical thickness [Bearden et al., 2006, 2009] and reduced gyrification [Schaer et al., 2009a] measured by local gyrification index [lGI, Schaer et al., 2008].

There is also emerging evidence of an atypical neurodevelopmental trajectory in 22q11.2DS, indicating changes in brain structure with age. Gothelf et al. [2007] reported significant reductions in cranial and cerebellar WM volume in children with 22q11.2DS relative to TD children in a 5-year period from middle childhood to late teen years. Schaer et al. [2009b] reported an atypical developmental trajectory of cortical complexity in a cross-sectional population of 6–40-year-old individuals with 22q11.2DS. Our study complements that study by hypothesizing differences in cortical gyrification in 6–15-year-old children with 22q11.2DS and typical controls. We also test the hypothesis that lGI will show an atypical developmental trajectory in the 22q11.2DS group, particularly in parietal, temporoparietal, and frontal regions, associated, in typically developing (TD) individuals, with visuospatial, attentional, and numerical functions.

MATERIALS AND METHODS

Imaging Data

T1-weighted structural images were acquired on a 3T Siemens Trio MRI System (Siemens Healthcare, Erlangen, Germany) using a magnetization prepared rapid gradient echo (MPRAGE) pulse sequence (voxel resolution = 1 mm^3, matrix size = 256 × 256, slice direction = sagittal,

number of imaged slices = 192, TR = 2170 ms, TE = 4.82 ms, and flip angle = 7°). The T1-weighted structural images from a total of 86 participants (6–15-year-old) were used for the structural data analysis. Of these participants, 49 children (mean ± standard deviation for age: 10.74 ± 1.69 years) had a confirmed diagnosis of 22q11.2DS, based on a positive standard fluorescence *in situ* hybridization test (FISH) for the deletion, and 37 children in the same age range (mean age: 10.27 ± 2.40 years) were TD, and participated as controls. Before scanning, all children were familiarized with the scanner environment in a full-size mock scanner and also were trained to suppress head motion. In all 86 participants scanned, no significant motion artifacts occurred in the T1-weighted images, exemplifying the effectiveness of this training for this atypical population. The training enabled us to include all the acquired images in the structural data analysis.

Structural Data Analysis

The MPRAGE images were processed using the workflow provided by the freely available software, FreeSurfer (http://surfer.nmr.mgh.harvard.edu/). The processing involved standard preprocessing including removal of bias field-induced intensity inhomogeneities, skull-stripping, and registration to Talairach coordinate system. By design, the freeSurfer software processes each hemisphere individually. The image processing most relevant to our specific analysis was the generation of a tessellated cortical surface model [Dale and Sereno, 1993; Fischl and Dale, 2000] to accurately replicate the gray-white matter and gray-pial interface. Once the cortical model was generated, a number of deformable procedures were performed including surface inflation [Fischl et al., 1999a], and registration to a spherical atlas that utilized individual cortical folding patterns to match cortical geometry across participants [Fischl et al., 1999b]. After the images from all participants were processed as described above, an unbiased population-specific template was generated in the standard space by averaging the surfaces from an equal number of controls and participants with 22q11.2DS (74 children total). The lGI was calculated on the mesh representation of the pial surface (a representation of cortical geometry) of each participant in the native space, as described in Schaer et al. [2008]. The process first involved generating an outer volume, obtained by morphological closing of the binarized representation of the pial mesh. The resulting volume was converted to its mesh representation, yielding an outer surface. lGI was then calculated for each vertex on this outer surface, as a ratio of areas of circular surface patches (regions of interest, ROIs) centered on this vertex and the area of the corresponding ROI on the pial surface. Hence, at each point, the lGI quantified, on the outer surface, the amount of cortex buried within the sulcal folds in its vicinity [Schaer et al., 2008]. As a final step, the lGI values on the outer surface were propagated to the

pial surface using a degressive weighing scheme (for details of this step, see Schaer et al., 2008], resulting in a map of the lGI on each vertex on the pial surface of each brain. The resulting lGI map on the pial surface of each brain was then sampled to the common average spherical coordinate system. The data on the pial surface was smoothed by a surface-based Gaussian smoothing kernel [Hagler et al., 2006] of FWHM = 20 mm, before statistical analysis. Additionally, total cortical volume was extracted from the volumetric quantification reported by Freesurfer, as the sum of volumes of segmented cerebral gray matter structures, with partial volume correction. A general linear model (GLM) was fitted at each vertex, modeling lGI as a linear combination of the categorical diagnosis variable (DX = control or 22q11.2DS), the age, and the total cortical volume. Spatially extended statistical parameter maps (SPMs), specifically T-score maps, of contrasts addressing appropriate hypotheses under examination were evaluated for regionally specific effects. Thresholding was performed based on peak height and cluster extent determined by random field theory [Worsley et al., 1996] and modified for Gaussian fields on manifolds [Taylor and Adler, 2003]. For anatomically meaningful visualization and reporting of significant clusters, the clusters were mapped to a sulcal-and gyral-based cortical parcellation atlas provided by Freesurfer [Fischl et al., 2004], and percentage overlaps of labeled anatomical regions with the cluster were calculated and tabulated.

RESULTS

Group Differences

To evaluate group differences in lGI within the study population, a standard groupwise GLM-based analysis was performed between the TD and the 22q11.2DS groups. The design matrix was constructed to encode lGI as being linearly dependent on the categorical variable of diagnosis and the continuous variables of age and the total cortical volume. The parameter estimates of the model were then contrasted to test for significant differences between the groups based on diagnosis. Specifically, we hypothesized that we would detect cortical regions where the lGI for TD was greater than that for children with 22q11.2DS, while controlling for age and total cortical volume. Figure 1a shows widespread cortical areas of vertex level significant differences in lGI where values in the 22q11.2DS group were significantly lower than in TD children. Consistent with our hypothesis, the data showed these cortical areas lie mainly along the midline of the brain and also span multiple regions bilaterally along the mid-sagittal plane. To identify regionally specific areas of lGI reduction, a cluster level inference ($\alpha \leq 0.05$) was drawn from the suprathresholded SPM (Fig. 1b). MNI coordinates and descriptive statistics for this cluster are tabulated in Table I. The cortical areas that showed a regionally specific reduction in lGI in the 22q11.2DS group included the precuneus
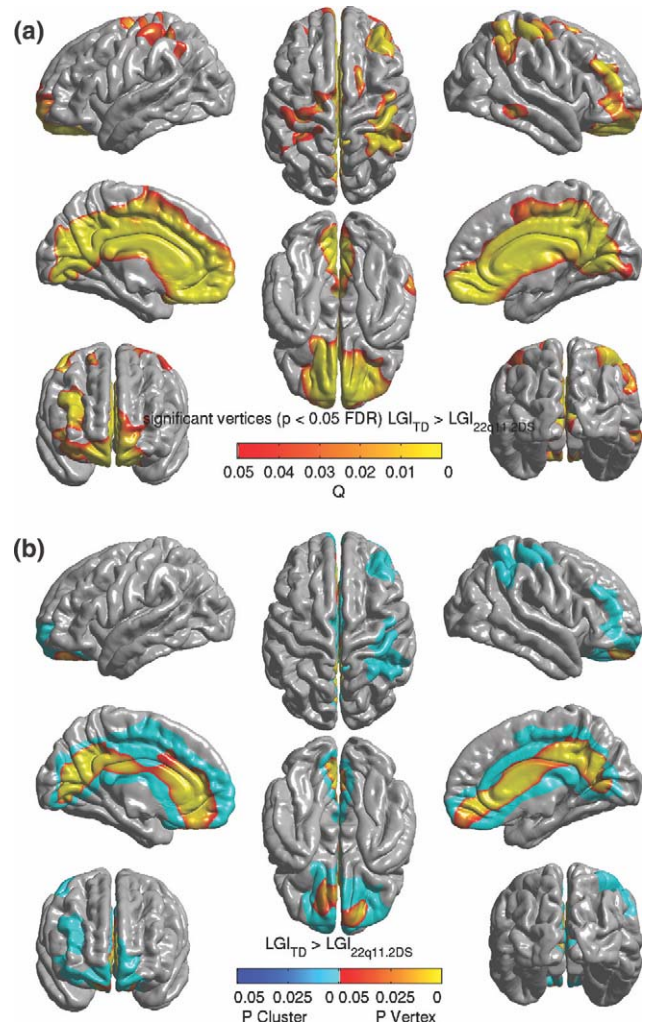
Figure 1.

Significant vertices and clusters where the lGI for TD was significantly greater than those for the 22q11.2DS population, controlling for age and cortical volume, and projected on the average pial surface of the population specific template. (**a**) Significant vertices explored with FDR-corrected SPM at $\alpha = 0.05$. *P*-values for suprathreshold voxels are color coded according to the hot color map. The image shows large bilateral areas of lGI decrease in 22q11.2DS population, involving most of the mid-line structures, and a bilateral ares of deficit involving the superior parietal, inferior parietal, central and superior precentral areas. (**b**) Only the significant vertices that were in the midline regions and right parietal/prefrontal areas were included in significant clusters, after thresholding for both the peak height and extent ($t \geq 4.01$, extent ≥ 0.52 resels). The *P*-values for the significant clusters, the entirety of which get a single *P* value, have been color coded in shades of blue. The coordinates of peak vertices within the clusters and other descriptive statistics are tabulated in Table I.

TABLE I. Details of vertex clusters of significant differences in LGI (TD > 22q11.2DS) after controlling for cortical volume and age

Hemisphere	SPM{t}	Size (resels)	MNIX	MNIY	MNIZ	P-value
Left	6.494	12.19	−5.59	−67.89	10.73	$5.\,25 \times 10^{-7}$
Right	5.999	11.62	0.14	19.20	−1.18	$5.\,27 \times 10^{-7}$
Right	4.076	3.19	47.81	−28.31	57.38	0.0013

The significant clusters were discovered after thresholding for both peak height and extent.

(lGI values were 20% lower), cuneus (30%), cingulate gyrus (Isthmus, 15%, Main part, 55%), cingulate sulcus (Main part and Intracingulate, 44%, Marginalis, 33%), and pericallosal sulcus (49%). Within the left hemisphere, the areas that showed significant lGI reductions in the 22q11.2DS group were the occipitotemporal gyrus (34%), parietooccipital sulcus (44%), subparietal sulcus (41%), and suborbital sulcus (69%). In the right hemisphere, the areas that showed significant lGI reductions were the frontal inferior gyrus (orbital and opercular part, 39 and 55%, respectively), inferior parietal gyrus (supramarginal, 53%), superior parietal gyrus (29%), subparietal sulcus, and transverse temporal sulcus. A complete list of cortical regions overlapping with the cluster determined by cluster-level inference, along with percentage overlap of the region with the cluster, is provided in Tables IV and V (columns 2 and 3).
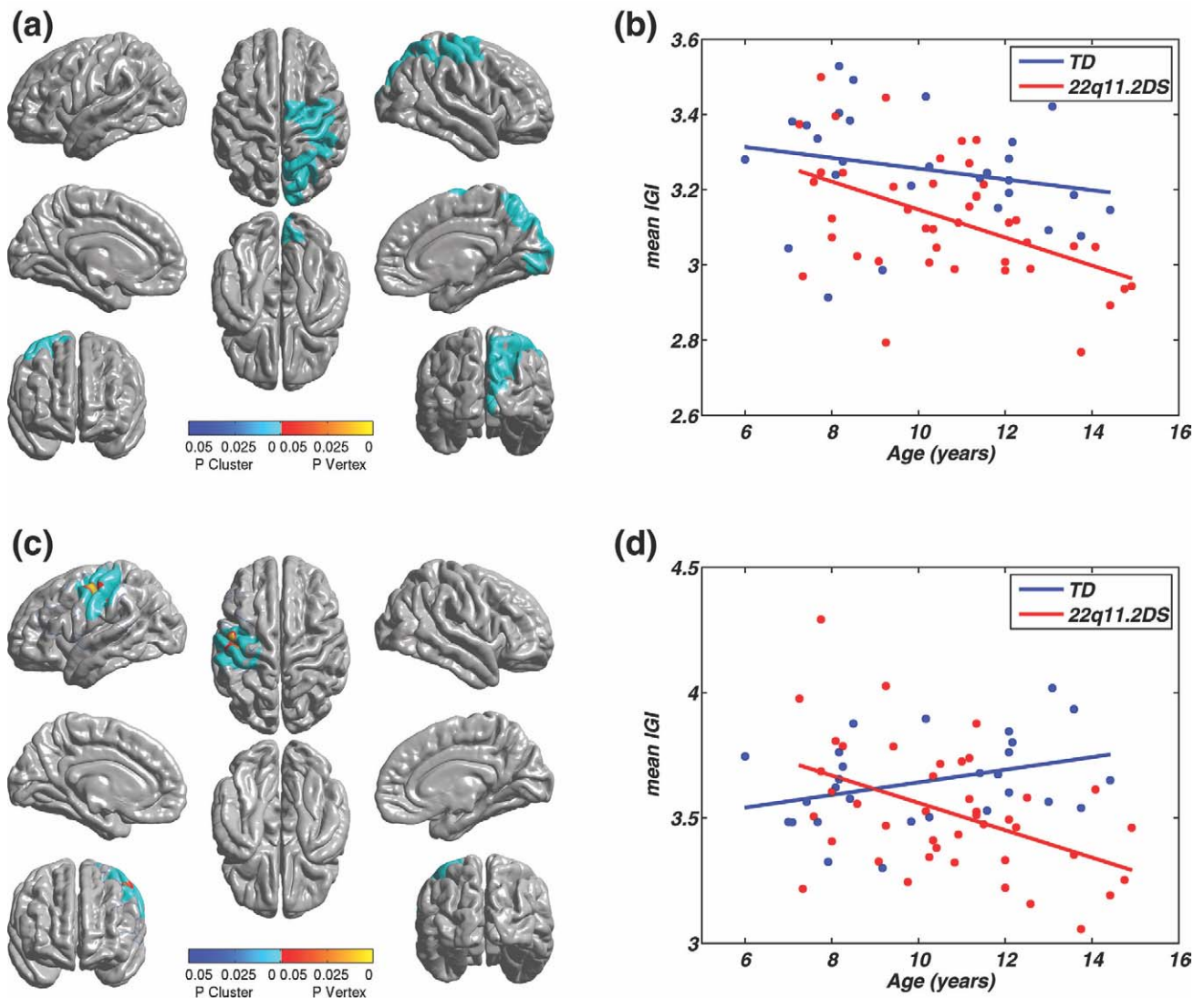
Age-Related lGI Changes

To evaluate our hypothesis that children with 22q11.2DS exhibit atypical developmental trajectory of cortical gyrification in specific regions over the age range of 6–15 years, we initially performed a linear regression with image data from children with 22q11.2DS and TD children combined. Here, age was selected as the independent variable to determine its linear relationship with lGI while controlling for total cortical volume. This main effect analysis revealed one significant cluster (Fig. 2a and Table II, first row), which showed a significant negative correlation between lGI and age ($T = -3.53$, $P = 0.001$). This cluster, located in the right hemisphere, included the paracentral gyrus (51%), superior parietal gyrus (35%), inferior parietal gyrus (37%), precuneus (30%), and transverse intraparietal and parietal sulcus (44%; Tables IV and V, columns 4 and 5). Using this cluster as a ROI, we split the analysis by diagnostic group (Fig. 2b) and found distinct trends within each group. The effect of age on lGI was not significant in the TD group ($T = -1.2206$, $P = 0.233$ n.s) but there was a significant negative correlation in the 22q11.2DS group ($T = -3.5$, $P = 0.001$). This different pattern of age dependence on lGI between the groups indicates a difference in the developmental trajectory of cortical gyrification, where both the groups show some decrease in lGI with age but the children with 22q11.2DS show significantly greater reductions between 6 and 15 years of age than TD children. Parts of this age-modulated cluster overlapped

the cortical areas where the lGI in children with 22q11.2DS was significantly reduced independently of age (Fig. 1b). Common regions included the paracentral gyrus, inferior and superior parietal gyrus, subparietal sulcus, and the sulci in the central insula.

Given the observed differences in age-modulated lGI between groups in this one cluster, we next tested the entire cortical surface for areas where the linear relationships between age and lGI were significantly modulated by the diagnosis. This was done by extending the GLM to include an interaction term. Figure 2c shows the cortical location of the resulting cluster, that is, where the interaction of age with diagnosis was significant. The anatomical location of the peak of this cluster was approximately contralateral to the peak of the cluster encompassing the main effect (Table II, second row). This cluster included supramarginal part of the inferior parietal gyrus (10%), postcentral gyrus (44%), precentral gyrus (27%), central sulcus (25%), postcentral sulcus (29%), and superior part of the precentral sulcus (33%). In this cluster (Fig. 2d), the mean lGI values in the TD children showed an increase with age, whereas those in children with 22q11.2DS showed a decrease, leading to a significant interaction ($F = 12.78$, $P = 0.001$). There was no overlap between the clusters showing this significant interaction and clusters showing significant group differences in lGI. However, some voxels in the interaction cluster did overlap with those significant in vertex level main effect SPM. These were in the central sulcus and precentral gyrus in the left hemisphere (Fig. 1a). Anatomically, the interaction reveals cortical areas where the TD children showed a moderate (n.s) increase in cortical gyrification with age but children with 22q11.2DS showed significant reductions in cortical gyrification within the 6–15 years age range. This pattern of change in lGI over the 6–15 years interval, observed in the interaction, is also different from that observed in the main effect, in that the cortical areas in that analysis showed a moderate decrease in lGI with age TD children.

Figure 2d shows that the relative mean value of lGI in the observed cluster is different in the two groups at different ages. Specifically, lGI values in TD children are slightly lower than those for children with 22q11.2DS until ∼ 8 years of age. Then the reverse becomes true. To examine if significant differences existed at different points within the age 6–15-year-old age range between the two groups, we decided to examine mean lGI in this cluster within 3-year subdivisions of the age intervals. We defined

Figure 2.

Age-related lGI changes within and across groups. (**a**) On covarying for age in the pooled population (TD children and children with 22q11.2DS), a large regionally significant cluster was observed in the right hemisphere ($P = 1.3 \times 10^{-4}$), involving the dorsocentral and parietal cortex, and extending to the occipital regions. (**b**) A regression line plotted through mean lGI within this cluster, for all children, and split according to diagnosis, shows a significant negative linear correlation with age for the group consisting of children with 22q11.2DS ($T = -3.50$, $P = 0.001$). The negative relationship visible in the plot for the TD children was nonsignificant ($T = -1.22$, $p = 0.233$). With the diagnosis groups combined, an overall negative effect of age on lGI was observed ($T68 = -3.52$, $P = 0.001$). (**c**) Regionally significant cluster in the left hemisphere, where diagnosis significantly modulated the age related changes in lGI ($P = 1.07 \times 10^{-4}$). The cortical areas included in the cluster are inferior parietal gyrus, postcentral gyrus, precentral gyrus, central sulcus, postcentral sulcus, and superior part of precentral sulcus. (**d**) The age × diagnosis interaction depicted in (c) is illustrated by plotting the mean lGI in this cluster as a function of age and diagnosis. The coordinates of the peak vertices within the cluster, and other descriptive statistics are tabulated in Table II.

the groups as follows: "younger" (6–9 years), "middle" (9–12 years), and "older" (12–years) (Fig. 3a). Children with 22q11.2DS showed a larger decrease in mean lGI between the middle and older age range than between the younger to the middle age range. A similar trend in the TD children is also visible in Figure 3a (blue lines), though this rate of change in lGI appears to be more uniform across all age ranges. Hence, the interaction in Figure 2d suggests

TABLE II. Clusters showing a significant main effect of age and interaction between age (entire range) and diagnosis

Hemisphere	Effect	max (SPM{t})	Size (resels)	MNIX	MNIY	MNIZ	P-value
Right	Main	4.43	9.43	49.46	−19.24	60.62	0.00013
Left	Interaction	4.02	4.37	−49.99	−11.53	44.52	0.025

two distinct trends within each diagnosis group between 6 and 15 years of age. To quantify the presence of such effects over the entire cortical surface, we repeated the previous analysis of interactions, now comparing diagnosis within pairs of the younger, middle, and older age ranges (instead of the entire age range of 6–15 years). The only pair of age ranges that showed an age by diagnosis interaction was the youngest (6–9) versus the oldest (12–15) ranges. The cortical areas showing significant interactions were contained within two clusters, one in each hemisphere (Fig. 3b and Table III). Strikingly, these completely included the cluster showing the interaction over the entire age range (Fig. 2c). The sulci and gyri of the occipital cortex were included bilaterally in both the clusters. Within the left hemisphere, the inferior parietal gyrus (supramarginal part: 26% and angular part: 13%), postcentral gyrus (44%), precentral gyrus (32%), inferior and middle temporal gyrus (52 and 18%, respectively), central sulcus (40%), and inferior, superior, and transverse temporal sulcus (39, 36, and 26%, respectively) were included in the cluster. The cortical areas included within the right hemisphere were the paracentral gyrus (29%), superior parietal gyrus (26%), precuneus (47%), cuneus (33%), parieto-occipital sulcus (50%), and subparietal sulcus (42%). The parietal regions included in the right hemisphere also overlapped with the clusters showing significant group differences in lGI (Tables IV and V). The left hemisphere cluster also included the cluster that showed a significant age by diagnosis effect for the entire age range (i.e., 6–15 years, Fig. 2a). In summary, when we examined developmental trajectory more directly by examining the interaction of age and diagnosis in three smaller age ranges, we found the following complementary pattern. TD children showed a significant increase in mean lGI between the age ranges of 6–9 years and 9–12 years, in several cortical regions (Fig. 3c,d). By contrast, children with 22q11.2DS showed the opposite pattern of reduction in lGI in the same regions, many of which have been strongly associated with spatial, temporal, and numerical processing in TD individuals.

In other words, the cortical regions shown in Figure 3b identify a significant difference in the trajectory of cortical gyrification development between 6–15-year-old TD children and those with 22q11.2DS. Although lGI increased in the typical group, it declined in the 22q11.2DS group. More specifically, the existence of interactions in only two age ranges with the total 6–15-year span appears to identify the intermediate age range as the point at which development diverges. Examination of interactions within each age range did not show any significant effects, probably due to reduced power due to decreased sample size. However, when the two groups were pooled for just the 12–15 years age range, we did observe a significant negative correlation of lGI with age (Fig. 2a,b). Similar effects were not observed in any other age interval implying that the most salient change in lGI with age for children with 22q11.2DS is a decrease cortical gyrification within cortical areas in Figure 3b. Also, the decrease in cortical gyrification happens more rapidly in the older children with 22q11.2DS, when compared with the younger children with the deletion. As the TD children show an increase in lGI with age, this also indicates the existence of an atypical trajectory of cortical gyrificaton with age in children with 22q11.2DS, when compared with the TD children.

DISCUSSION

The lGI metric quantifies the geometry of the cortex and likely provides information about underlying connectivity. Recently, Meechan et al. [2009] experimentally demonstrated that diminished dosage of 22q11.2 genes disrupts neurogenesis and neuronal migration, implying altered cortical connectivity. Our findings of altered cortical gyrification in children with 22q11.2DS further implicate atypical connectivity. We focused on investigating whether an atypical developmental trajectory exists for cortical areas typically associated with the nonverbal cognitive impairments experienced by most children with 22q11.2DS [e.g., Simon, 2008]. As altered connectivity would impact information processing capabilities, atypical cortical gyrification might help to explain cognitive impairments associated with the disorder.

Recently, the trajectory of typical brain development has been mapped using longitudinal and cross-sectional measures of gray and white matter volume and cortical thickness. Studies report that distinct cortical areas show differently shaped developmental trajectories that are strongly influenced by the cytoarchitecture of the region [e.g., Lenroot and Giedd, 2006; Shaw et al., 2008]. Furthermore, alongside an overall gradual decrease in complexity of the TD cortex in both hemispheres between 6 and 16 years of age, some cortical areas show local complexity increases during this period [White et al., 2010]. This is consistent with our finding that the main effect of age from 6–15 years revealed widespread cortical areas where cortical complexity in typical children reduced slightly with age (Fig. 2a,b, blue line). These results indicate that
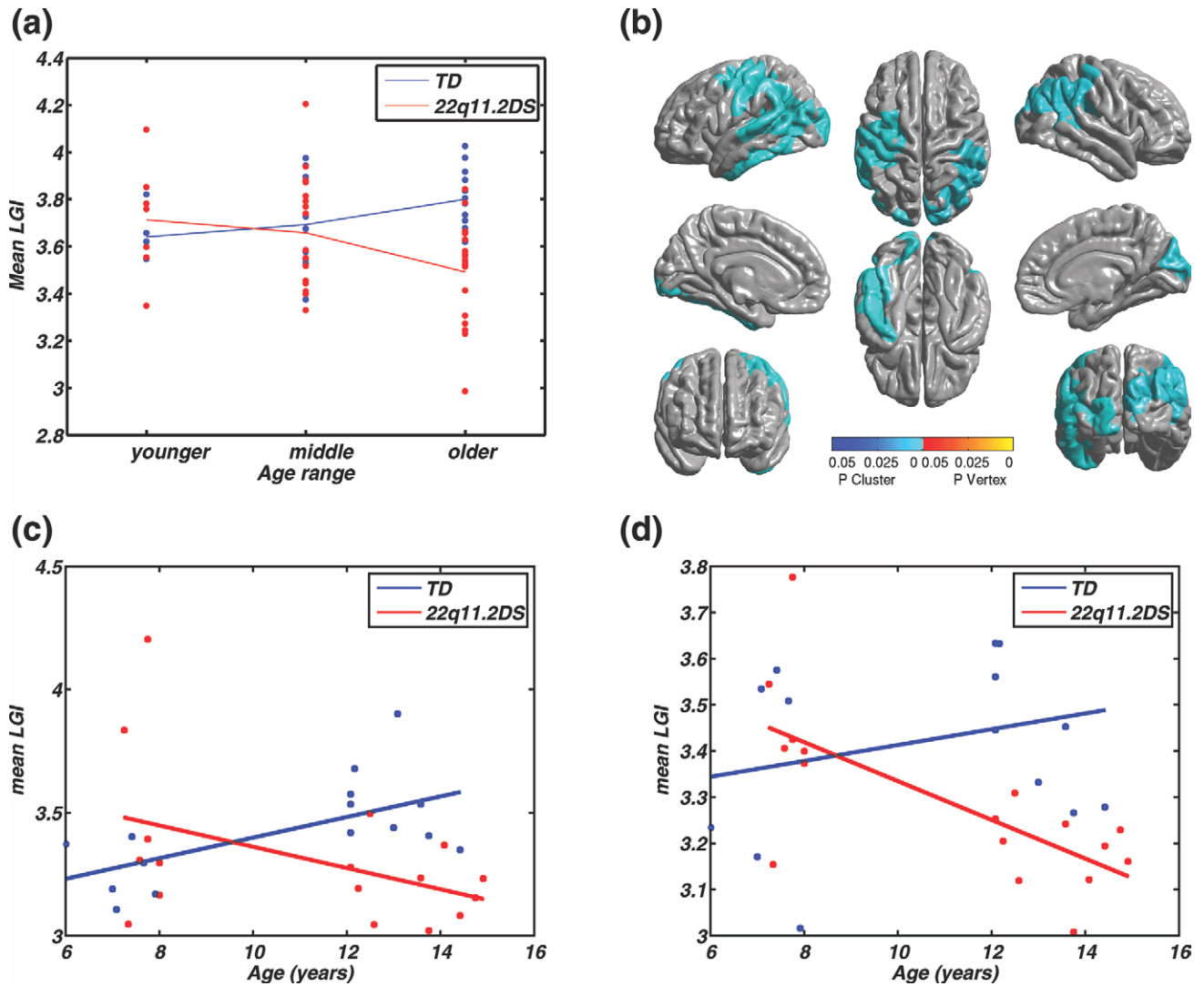
Figure 3.

(**a**) Main effect of age showing the mean lGI in the cluster in Figure 2b, split by diagnosis and age ranges of younger (6–9 years), middle (9–12 years) and older (12–15 years). Visually, the mean lGI changes differently across diagnosis groups, and across age ranges for children with 22q11.2DS, the mean lGI reduces by a greater amount between the middle and older group, when compared with that between younger and middle group. (**b**) Clusters showing significant interaction between age ranges and diagnosis, where the levels of age were from the younger and the older age range. The cortical areas showing opposite patterns of age-related changes in cortical gyrification in TD chil-dren and in children 22q11.2DS are spread across both the hemispheres. The parietal aspect of the cortex is involved bilaterally. The left hemisphere cluster also includes the superior/inferior temporal regions, whereas the right hemisphere includes the cuneus, among other regions, in which the lGI decreased significantly in the children with the deletion, when compared with the typical controls. (b) Plot of the mean lGI values in the left cluster as a function of age ($F(1,28) = 9.01$, $P = 0.006$), (**c**) Plot of the mean lGI values in the right cluster as a function of age ($F(1,28) = 8.39$, $P = 0.007$). MNI coordinates and other descriptive statistics have been tabulated in Table III.

the typical cortex undergoes regionally specific changes in cortical folding during childhood and adolescence, which may arise from development of intracortical connections [Rakic, 1988]. Notably, the children with 22q11.2DS do not demonstrate this developmental trajectory.

The most extensive age-independent group differences children were bilaterally situated along the midline, where the children with 22q11.2DS showed reduced cortical gyrification (Fig. 1b). These clusters are colocalized to our previous report of significant alterations in midline

TABLE III. Details of the clusters that showed significant interaction between diagnosis and age ranges of younger and older (Fig. 3)

Hemisphere	Effect	max (SPM{t})	Size (resels)	MNIX	MNIY	MNIZ	P-value
Left	Interaction	3.89	16.13	−44.48	−15.44	43.37	2.52×10^{-5}
Right	Interaction	3.06	7.56	46.36	−56.97	28.49	0.0029

No significant correlations or interactions were discovered in any other age interval and pair of age intervals, respectively.

TABLE IV. Cortical parcellations that overlap with the significant clusters discovered by the various contrasts used in the study

Cortical areas overlapping with significant clusters	Contrasts						
	Group differences				Effect of Age		
			6–15 years		6–9 and 12–15 years		
			Main	Interaction	Main	Interaction	
Hemisphere	Left	Right	Right	Left	Right	Left	Right
G cingulate-Isthmus	15	0	0	0	0	0	12
G cingulate-Main part	55	0	0	0	0	0	31
G cuneus	30	0	0	0	0	0	33
G frontal inf-Opercular part	0	39	0	0	0	0	0
G frontal inf-Orbital part	0	55	0	0	0	0	0
G frontal inf-Triangular part	0	43	0	0	0	0	0
G frontal superior	17	2	5	0	0	0	0
G frontomarginal	20	22	0	0	0	0	0
G insular long	0	14	0	0	0	0	0
G insular short	0	9	0	0	0	0	0
G and S occipital inferior	0	0	0	0	39	7	0
G occipital middle	0	0	27	0	28	28	38
G occipital superior	0	0	3	0	0	5	44
G occipit-temp lat-Or fusiform	0	0	0	0	9	21	0
G occipit-temp med-Lingual part	34	0	0	0	0	11	4
G orbital	19	18	0	0	0	0	0
G paracentral	4	45	51	0	0	0	29
G parietal inferior-Angular part	0	11	37	0	31	13	11
G parietal inferior-Supramarginal part	0	53	0	10	0	26	0
G parietal superior	0	29	35	0	1	3	26
G postcentral	0	16	5	44	0	44	0
G precentral	0	9	27	27	0	32	3
G precuneus	20	35	30	0	0	0	47
G rectus	51	0	0	0	0	0	0
G subcallosal	41	0	0	0	0	0	0
G subcentral	0	37	0	5	0	10	0
G temporal inferior	0	6	12	0	8	52	1
G temporal middle	0	28	4	0	1	18	1
G temp sup-G temp transv and interm S	0	34	0	0	0	22	0
G temp sup-Lateral aspect	0	21	0	0	0	27	0
G temp sup-Planum tempolare	0	55	0	0	0	43	0
G and S transverse frontopolar	31	18	0	0	0	0	0
Lat Fissure-ant sgt-ramus horizontal	0	46	0	0	0	0	0
Lat Fissure-ant sgt-ramus vertical	0	59	0	0	0	0	0
Lat Fissure-post sgt	0	45	0	0	0	16	0
Medial wall	17	0	0	0	0	0	1

The cortical parcellations are as defined in Fischl et al. (2004). Only cortical area which are included in at least one cluster are presented in table, though the parcellations report 82 distinct regions. In each case, the numbers in the cell report what percentage of the cortical area, designated in the rows, overlapped with the significant cluster discovered by the contrast specified along the columns.

TABLE V. Cortical parcellation overlapping with significant clusters, continued from Table IV

	Contrasts						
	Group differences 6–15 years				Effect of Age 6–9 and 12–15 years		
			Main	Interaction	Main	Interaction	
Cortical areas overlapping with significant clusters	Left	Right	Right	Left	Right	Left	Right
Pole occipital	0	0	0	0	0	29	0
Pole temporal	0	0	0	0	0	20	0
S calcarine	42	0	0	0	0	0	26
S central	0	10	25	36	0	40	6
S central insula	0	24	25	36	0	40	6
S cingulate-Main part and Intracingulate	44	0	0	0	0	0	1
S cingulate-Marginalis part	33	8	18	0	0	0	34
S circular insula anterior	0	20	0	0	0	0	0
S circular insula inferior	0	12	0	0	0	2	0
S circular insula superior	0	54	0	0	0	8	0
S collateral transverse ant	0	0	0	0	0	45	0
S collateral transverse post	0	0	0	0	0	14	0
S frontomarginal	13	28	0	0	0	0	0
S intermedius primus-Jensen	0	42	0	0	0	42	0
S intraparietal-and Parietal transverse	0	2	44	0	17	8	11
S occipital anterior	0	5	31	0	47	53	47
S occipital middle and Lunatus	0	0	20	0	3	51	30
S occipital superior and transversalis	0	0	28	0	20	12	46
S occipito-temporal lateral	0	0	8	0	28	46	0
S orbital-H shaped	21	30	0	0	0	0	0
S orbital lateral	0	39	0	0	0	0	0
S orbital medial-Or olfactory	38	0	0	0	0	0	0
S paracentral	8	8	48	0	0	0	0
S parieto occipital	44	0	0	0	0	0	50
S pericallosal	49	0	0	0	0	0	18
S postcentral	0	20	2	29	0	45	0
S precentral-Superior-part	0	6	33	33	0	46	0
S subcentral ant	0	15	0	0	0	0	0
S subcentral post	0	48	0	0	0	2	0
S suborbital	69	0	0	0	0	0	0
S subparietal	41	22	15	0	0	0	42
S temporal inferior	0	9	11	0	12	39	3
S temporal superior	0	26	8	0	11	36	5
S temporal transverse	0	54	0	0	0	26	0

morphology derived from VBM of brain tissue volume, and, to a lesser extent, fractional anisotropy anomalies [Simon et al., 2005]. Gray matter volume reductions in 22q11.2DS have also been reported [Campbell et al., 2006; Shashi et al., 2009] in some of the midline structures that showed reduced lGI in our population (the right cuneus, right middle, inferior frontal, and right anterior cingulate). Central midline structures have been functionally linked to a range of cognitive impairments strongly associated with 22q11.2DS, less transient cognitive operations involving the sense of self [Northoff and Brempohl, 2004; Simon et al., 2005], and some behavioral and psychiatric disorders reported in the 22q11.2DS population [Gothelf et al., 2007; Schaer et al., 2009].

The parietal regions in which we detected group differences are critical to a range of typical visuospatial attention, comparative and numerical functions, which are domains of particular cognitive impairment in 22q11.2DS. Also, an fMRI study by Eliez et al. [2001] indicated that functional activations of inferior parietal cortex in a small group of participants with 22q11.2DS of a similar age to those in our study were atypical when solving difficult math problems. Also, atypical FA values in the white matter tracts subserving the right parietal regions have been linked to higher cost of redirecting attention to targets in face of invalid cues in a spatial attention task [Simon et al., 2008]) and to impaired arithmetical abilities [Barnea-Goraly et al., 2003].

As examining the effect of age on changes in lGI could reveal critical neurodevelopmental aspects of cortical gyrification and the way its developmental trajectory might be modulated by chromosome 22q11.2 deletions, we carried out extensive cross-sectional analyses on our data. By pooling across diagnosis (Fig. 2a), we found several cortical areas in the right hemisphere where lGI correlated significantly and negatively with age, suggesting that complexity might decrease regionally with age in these right hemisphere cortical areas. However, post hoc analyses that examined the trends separately in the diagnosis groups (Fig. 2b), showed that the decrease in lGI in this cluster with age was only significant in children with 22q11.2DS. This implies that the developmental trajectory of cortical gyrification is atypical in children with 22q11.2DS in that it reduces significantly more with age than in TD children in these cortical areas. Among the areas included in the cluster that overlapped with regions of significant group difference in lGI (Fig. 1b) were the paracentral gyrus, the inferior parietal gyrus (angular gyrus, AG and supramarginal gyrus, SMG), and the central insula. The remaining extent of the cluster, that is, voxels not overlapping with the group difference main effect, mainly included the intraparietal sulcus and parts of posterior parietal lobe frequently associated with attentional, comparative, and numerical functioning.

A second cluster, in the left hemisphere (Fig. 2c), also showed different trajectories in the two groups. Here, lGI values in the 22q11.2DS group showed a significant decrease with age, whereas those in the TD group increased between the ages of 6–15 years (Fig. 2d). The cortical areas involved included the central sulcus, central insula, precentral, and postcentral cortex. These cortical gyrification differences were not evident when age was not considered (Fig. 1) but do appear as an age by diagnosis interaction. They depict an atypical negative developmental trajectory in the 22q11.2DS group compared with the typical positive pattern of change, which is consistent with the definition of the left parieto-occipital lobe of Blanton et al. [2001] that showed a positive linear increase in cortical complexity with age for young subjects.

In addition to showing these larger differences in developmental trajectory, we also reported that the amount of change in lGI values varied differently within the entire age range we studied (Fig. 3a). When the full age range was split into 3-year intervals (younger, middle, and older), significant interactions between age range and diagnosis were found only when comparing the younger and the older age ranges (Fig. 3b–d). Several differences are evident from Figure 3a. The first is that the direction of gyrification change is different for the two groups; that is, increasing in the TD group and decreasing in the 22q11.2DS group. The second is that the amount of change is much greater between the middle and oldest age range than between the youngest and middle age range. This difference is what creates the significant statistical interaction between lGI and age in our analyses. In neurodevelopmental terms, this indicates that in some brain regions, there was a significant reduction in cortical complexity between the ages of 9 and 15 years of age in almost all children with 22q11.2DS in our study, whereas those same regions showed a significant increase in cortical complexity in almost of the TD children in our study. The cortical areas showing this interaction are spread bilaterally and include precentral and postcentral, parietal, occipital cortex, temporal pole, and most of the cingulate gyrus. As already noted, most of these areas are of significant functional relevance based on what is known about the cognitive and behavioral characteristics of children with 22q11.2DS.

The neuromechanical hypothesis [Van Essen, 1997] relates cortical gyrification to underlying connectivity, which in turn has been shown to be atypical in children with 22q11.2DS [Barnea-Goraly et al., 2003; Simon et al., 2008] and related to performance in visuospatial attention tasks [Simon et al., 2008] and math reasoning [Barnea-Goraly et al., 2005]. Hence, cortical gyrification and its atypicality in 22q11.2DS can be linked, through this connectivity hypothesis, to the visuospatial, neurocognitive, and numerical impairments associated with the disorder. As a great deal of postnatal cortical development appears to be in terms of changes in connectivity, as indicated by extended increases in white matter volume [e.g., Lenroot and Giedd, 2006], gyrification might be expected to show a corresponding change between 6 and 15 years of age. The cortical areas showing atypical gyrification that we report largely consist of those implicated in the typical functioning of visuospatial attention and numerical cognition. Our results also demonstrate that these regions undergo an atypical developmental trajectory in children with 22q11.2DS, particularly, during the middle to later years of childhood when white matter volumes are increasing most [Lenroot and Giedd, 2006] and when parietal morphology is undergoing most sculpting in typical children [Gogtay et al., 2004]. The proximity of these clusters reported here to those in our DTI findings [Simon et al., 2008], particularly in the parietal lobe, further support the idea that these cortical complexity differences are associated with atypical development of underlying connectivity. Further research will validate these interpretations through longitudinal studies and may help to identify cognitive functions, cortical targets, and developmental timepoints for effective neurotherapeutic interventions.

ACKNOWLEDGMENTS

REFERENCES

Barnea-Goraly N, Menon V (2003): Investigation of white matter structure in velocardiofacial syndrome: A diffusion tensor imaging study. Am J Psychiatry 160:1863–1869.

Barnea-Goraly N, Eliez S, Menon V, Bammer R, Reiss AL (2005): Arithmetic ability and parietal alterations: A diffusion tensor

imaging study in velocardiofacial syndrome. Cogn Brain Res 25:735–740.

Blanton RE, Levitt JG, Thompson PM, Narr KL, Capetillo-Cunliffe L, Nobel A, Singerman JD, McCracken JT, Toga AW (2001): Mapping cortical asymmetry and complexity patterns in normal children. Psychiatry Res Neuroimaging 107:29–43.

Campbell LE, Daly E, Toal F, Stevens A, Azuma R, Catani M, Ng V, van Amelsvoort T, Chitnis X, Cutter W, Murphy DGM, Murphy KC (2006): Brain and behavior in children with 22q11.2 deletion syndrome: A volumetric and voxel-based morphometry MRI study. Brain 129:1218–1228.

Dale A, Sereno M (1993): Improved localization of cortical activity by combining EEG and MEG with MRI cortical surface reconstruction: A linear approach. J Cogn Neurosci 5:162–176.

Eliez S, Blasey C, Menon V, White C, Schmitt J, Reiss A (2001): Functional brain imaging study of mathematical reasoning abilities in velocardiofacial syndrome. Genet Med 3:49–55.

Eliez S, Schmitt JE, et al. (2000): Children and adolescents with velocardiofacial syndrome: A volumetric study. Am J Psychiatry 158:409–415.

Fischl B, Sereno M, Dale A (1999a): Cortical surface based analysis II: Flattening, and a surface based coordinate system. NeuroImage 9:195–207.

Fischl B, Sereno M, Tootell R, Dale AM (1999b): High-resolution intersubject averaging and a coordinate system for the cortical surface. Hum Brain Mapp 8:272–284.

Fischl B, Dale A (2000): Measuring the thickness of the human cerebral cortex from magnetic resonance images. Proc Natl Acad Sci USA 97:11050–11055.

Fischl B, Van der Kouwe A, Destrieux C, Halgren E, Sgonne F, Salat DH, Busa E, Seidman LJ, Goldstein J, Kennedy D, Caviness V, Makris N, Rosen B, Dale AM (2004): Automatically parcellating the human cerebral cortex. Cereb Cortex 14:11–22.

Giedd J (1999).Brain development, ix: human brain growth. Am J Psychiatry 156:4.

Gothelf D, Pennimanc L, Guc E, Eliez S, Reiss AL (2007): Developmental trajectories of brain structure in adolescents with 22q11.2 deletion syndrome: A longitudinal study. Schizophr Res 96:72–81.

Gogtay N, Giedd JN, Lusk L, Hayashi KM, Greenstein D, Vaituzis AC, Nugent TF, Herman DH, Clasen LS, Toga AW, Rapoport JL, Thompson PM (2004): Dynamic mapping of human cortical development during childhood through early adulthood. Proc Natl Acad Sci USA 101:8174–8179. Available at: http://dx.doi.org/10.1073/pnas.0402680101.

Gothelf D, Feinstein C, Thompson T, Gu E, Penniman L, Stone EV, Kwon H, Eliez S, Reiss AL (2007): Risk factors for the emergence of psychotic disorders in adolescents with 22q11.2 deletion syndrome. Am J Psychiatry 164:663–669. Available at: http://dx.doi.org/10.1176/appi.ajp.164.4.663.

Johnson MH (2001): Functional brain development in humans. Nat Rev (Neuroscience) 2:475–483.

Kates W, Burnette C, et al. (2001): Regional cortical white matter reductions in velocardiofacial syndrome: A volumetric MRI analysis. Biol Psychiatry 49:677–684.

Kobrynski L, Sullivan K (2007): Velocardiofacial syndrome, digeorge syndrome: The chromosome 22q11.2 deletion syndromes. Lancet 370:1443–1452.

Lenroot RK, Giedd JN (2006): Brain development in children and adolescents: Insights from anatomical magnetic resonance imaging. Neurosci Biobehav Rev 30:718–729. Available at: http://dx.doi.org/10.1016/j.neubiorev.2006.06.001.

Maynard T, Haskell G, Peters A, Sikich L, Liberman J, LaMantia A (2003): A comprehensive analysis of 22q11 gene expression in the developing and adult brain. Proc Nat Acad Sci USA 100:14433–14438.

McDonald-McGinn D, LaRossa D, GoldMutz E, Sullival K, Eicher P, Gerdes M, Moss E, Solot C, Schultz P, et al. (1997): The 22q11.2 deletion: Screening, diagnostic workup and outcome of results; Report on 181 patients. Genet Test 1:99–108.

Meechan DW, Tucker ES, Maynard TM, LaMantia A-S (2009): Diminished dosage of 22q11 genes disrupts neurogenesis and cortical development in a mouse model of 22q11 deletion/DiGeorge syndrome. PNAS 106:16434–16445.

Northoff G, Brempohl F (2004): Cortical midline structures and the self. Trends Cogn Sci 8:102–107.

Rakic P (1988): Specification of cerebral cortical areas. Science 241:170–176.

Schaer M, Schmitt JE, Glaser B, Lazeyeas F, Delavelle J (2006): Abnormal patterns of cortical gyrification in velo-cardio-facial syndrome (deletion 22q11.2): An MRI study. Psychiatry Res Neuroimaging 146:1–11.

Schaer M, Caudra MB, Tamarit L, Lazeyras F, Eliez S, Thiran J-P (2008): A surface-based approach to quantify local cortical gyrification. IEEE Trans Med Imaging 27:161–170.

Schaer M, Glaser B, Caudra MB, Debbane M, Thiran J-P, Eliez S (2009): Congenital heart disease affects local gyrification in 22q11.2 deletion syndrome. Dev Med Child Neurol.

Shashi V, Kwaplic T, Kaczorowskic J, Berryb M, Santos C, Howard T, Goradia D, Prasad K, Vaibhav D, Rajarethinam R, Spence E, Keshavan M (2009): Evidence of gray matter reduction and dysfunction in chromosome 22q11.2 deletion syndrome. Psychiatry Res Neuroimaging 181:1–8.

Shaw P, Kabani NJ, Lerch JP, Eckstrand K, Lenroot R, Gogtay N, Greenstein D, Clasen L, Rapoport JL, Giedd JN, Wise SP (2008): Neurodevelopmental trajectories of the human cerebral cortex. J Neurosci 28:3586–3594.

Shprintzen RJ (2000): Velocardiofacial syndrome. Otolaryngol Clin North Am 33:1217–1240.

Shprintzen RJ (2008): Velo-cardio-facial syndrome: A distinctive behavioral phenotype. Ment Retard Dev Disabil Res Rev 6:142–147.

Simon TJ, Ding L, Bish JP, McDonald-McGinn DM, Zackai EH, Gee J (2005): Volumetric, connective and morphologic changes in the brains of children with chromosome 22q11.2 deletion syndrome: An integrative study. Neuroimage 25:169–180.

Simon TJ, Burg-Malki M, Gothelf D (2007): Cognitive and behavioral characteristics of children with 22q11.2 deletion syndrome. In: Ross JL, Mazzocco MMM, editors. Neurogenetic Developmental Disorders: Manifestation and Identification in Childhood. Cambridge, MA: MIT press. pp 297–334.

Simon TJ, Wu Z, Avants B, Zhang H, Gee JC, Stebbins GT (2008): Atypical cortical connectivity and visuospatial cognitive impairments are related in children with chromosome 22q11.2 deletion syndrome. Behav Brain Funct 4.

Taylor J, Adler R (2003): Euler characteristics for Gaussian fields on manifolds. Ann Probab 31:533–563.

Van Essen DC (1997): A tension based theory of morphogenesis and compact wiring in the central nervous system. Nature 385:313–318.

White T, Su S, Schmidt M, Kao C-Y, Sapiro G (2010): The development of gyrification in childhood and adolescence. Brain Cogn 72:36–45.

Worsley K, Marrett S, Neelin P, Vandal A, Friston K, Evans A (1996): A unified statistical approach for determining significant signals in images of cerebral activation. Hum Brain Mapp 4:58–73.